Internet Electronic Journal of Molecular Design **2003**, *2*, 86–95 ISSN 1538–6414
BioChem Press http://www.biochempress.com

Internet Electronic Journal of Molecular Design

February 2003, Volume 2, Number 2, Pages 86–95

Editor: Ovidiu Ivanciuc

Special issue dedicated to Professor Haruo Hosoya on the occasion of the 65th birthday
Part 6

Guest Editor: Jun–ichi Aihara

Partial Structures of C_{60} Responsible for Its Lowest Electronic Absorption Band: Corannulene or Triphenylene?

Tai–ichi Shibuya,[1] Susumu Narita,[1] Yasushi Nomura,[1] and Tetsuo Morikawa[2]

[1] Department of Chemistry, Faculty of Textile Science and Technology, Shinshu University, Ueda, Nagano–ken, 386–8567, Japan
[2] Department of Chemistry, Joetsu University of Education, Joetsu, Niigata–ken, 943–8512, Japan

Received: October 21, 2002; Revised: November 22, 2002; Accepted: December 15, 2002; Published: February 28, 2003

Citation of the article:
T. Shibuya, S. Narita, Y. Nomura, and T. Morikawa, Partial Structures of C_{60} Responsible for Its Lowest Electronic Absorption Band: Corannulene or Triphenylene?, *Internet Electron. J. Mol. Des.* **2003**, *2*, 86–95, http://www.biochempress.com.

Inter*net* Electronic Journal of Molecular Design

BioChem Press
http://www.biochempress.com

Partial Structures of C_{60} Responsible for Its Lowest Electronic Absorption Band: Corannulene or Triphenylene?[#]

Tai–ichi Shibuya,[1,*] Susumu Narita,[1] Yasushi Nomura,[1] and Tetsuo Morikawa[2]

[1] Department of Chemistry, Faculty of Textile Science and Technology, Shinshu University, Ueda, Nagano–ken, 386–8567, Japan
[2] Department of Chemistry, Joetsu University of Education, Joetsu, Niigata–ken, 943–8512, Japan

Received: October 21, 2002; Revised: November 22, 2002; Accepted: December 15, 2002; Published: February 28, 2003

Internet Electron. J. Mol. Des. **2003**, *2* (2), 86–95

Abstract

Motivation. Corannulene is widely accepted as a particularly important fragment of the fullerene C_{60}. We consider that corannulene alone cannot explain the origin of the lowest–allowed electronic absorption band of C_{60}. Here we clarify what else is needed other than corannulene, and propose triphenylene as a more important partial structure of C_{60} for the electronic absorption.

Method. Full SECI calculations are made in the semiempirical CNDO/S approximation. We first observe how the degenerated MO–energy levels of C_{60} split as the molecular symmetry I_h breaks into two different elongated shapes, D_{5d} with its C_5–axis through a pair of corannulene parts and D_{3d} with its C_3–axis through a pair of triphenylene parts.

Results. Components of the molecular orbitals of C_{60} that play principal roles in the lowest–allowed electronic absorption are all found in the vicinity of the HOMO–LUMO gap of triphenylene, whereas some part is missing in corannulene. The lowest–allowed electronic transitions of larger triphenylene derivatives tend to converge to the lowest absorption band of C_{60}.

Conclusions. A pair of triphenylene molecules separated by the diameter of C_{60} in the staggered conformation (D_{3d}) makes a good model system to explain the origin of the lowest–allowed absorption band of C_{60}. As the C_{60} molecule has 20 equivalent 6–membered rings, there are ten choices for such a pair. On the other hand, a pair of corannulene molecules in the staggered conformation (D_{5d}) lacks one component of the HOMO of C_{60}, which we have found in the encircled *cis*–polyene of ten ethylene units at the equatorial belt of C_{60}.

Keywords. Fullerene C_{60}; absorption spectrum; triphenylene; corannulene; semiempirical MO method.

Abbreviations and notations

AM1, Austin model 1
CNDO/S, complete neglect of differential overlap, for spectroscopic use
CSF, configuration state function
HOMO, highest occupied MO
INDO, intermediate neglect of differential overlap
LUMO, lowest unoccupied MO
RPA, random–phase approximation
MO, molecular orbitals
SCF–MO, self–consistent field MO
SECI, singly–excited configuration interaction

[#] Dedicated to Professor Haruo Hosoya on the occasion of the 65th birthday.

* Correspondence author; E–mail: shibuya@giptc.shinshu–u.ac.jp.

1 INTRODUCTION

After fifteen years since the discovery of fullerene–C_{60} [1], chemists finally succeeded in synthesizing it by rational chemical methods [2,3]. On the other hand, the understanding of the characteristic absorption spectrum of C_{60} in the full range of 200 nm – 400 nm is still far from satisfactory. However, the lowest–energy band that peaks at *ca.* 3.8 eV (325 nm) has been unambiguously assigned to the lowest allowed transition $1^1A_g \rightarrow 1^1T_{1u}$ which is essentially due to excitations of an electron from the highest occupied h_u–shell to the lowest unoccupied t_{1g}– and h_g–shells [4].

In this article we investigate the origin of the lowest allowed transition of C_{60} in relation to the two smallest fullerene fragments: corannulene and triphenylene. For this purpose we will consider simple model systems consisting of a pair of corannulene molecules and a pair of triphenylene or triphenylene–derivative molecules, all in the staggered conformation. The model system of corannulene therefore has the symmetry D_{5d}, and those of triphenylene and triphenylene derivatives have the D_{3d}, while the symmetry of C_{60} is I_h. In our simple model systems, interactions between paired molecules are ignored so that a photon is practically absorbed by a single molecule of corannulene, triphenylene, or its derivative. Therefore, SECI calculations will be made on single molecules rather than pairs of molecules. We will also discuss how the degenerate MO–energy levels of C_{60} split as the symmetry breaks from I_h to D_{5d} and D_{3d} along the C_5 and C_3 rotation axes, respectively (see Figure 1).

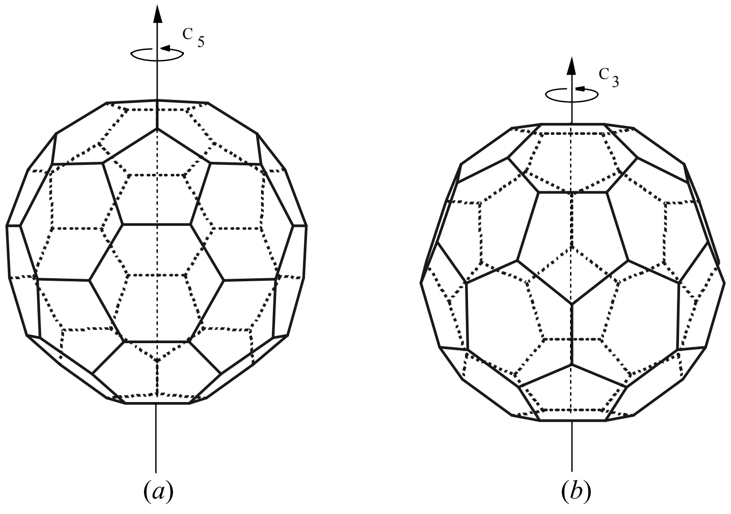

Figure 1. The fullerene C_{60}. (*a*) The C_5–rotation axis goes through the centers of a pair of pentagonal faces in the staggered conformation. The bisector vertical to the sheet is one of the five σ_d–planes around the C_5–axis; (*b*) The C_3–rotation axis goes through the centers of a pair of hexagonal faces in the staggered conformation. The bisector vertical to the sheet is one of the three σ_d–planes around the C_3–axis.

2 CALCULATION

All SCF–MO calculations and SECI calculations were made in the CNDO/S approximation [5–9]. All the singly–excited configurations were included in the SECI calculations. The computed results on C_{60} are taken from Ref. [4], where large–scale SECI matrices were reduced according to the irreducible representations of I_h by the use of the projection operators and the reduced matrices in much smaller sizes were diagonalized. The geometrical structures of the fullerene fragments used in the present calculations are those optimized with the molecular computational software MacSpartan [10] at the AM1 (Austin model 1) level [11].

In Ref. [4], we made calculations on C_{60} not only in the CNDO/S approximation but also in the INDO/S approximation. (See Ref. [12] for the INDO approximation and Refs. [13–15] for its spectroscopic parameterization.) The INDO/S results of excitation energies through the full SECI calculations were a little higher than the CNDO/S, but all within 3% for the allowed transitions. Therefore, in the present study, we adopt the CNDO/S as it is simpler and more commonly used than the INDO/S. The accuracy of the INDO/S–SECI method was checked by Feng *et al.* [16] on corannulene. Needless to say, more reliable methods, *e.g.*, *ab initio* calculations are desirable, but such a calculation is impracticable for the excited states of C_{60}, and in fact no successful *ab initio* calculation has been reported to date.

3 RESULTS AND DISCUSSION

In our earlier study [4], the full SECI calculation on C_{60} gave the lowest–allowed transition $1^1A_g \rightarrow 1^1T_{1u}$ at 3.47 eV (357 nm) with the oscillator strength $f = 0.34$. The weight of transitions of an electron from the highest occupied h_u–shell to the lowest unoccupied t_{1g}–shell was 0.49, and that to the lowest unoccupied h_g–shell was 0.30. The full RPA (random–phase approximation) calculation which takes into account a certain type of electron correlations that are missing in the SECI calculation gave it at 3.35 eV (370 nm) with $f = 0.54$. The weight was then 0.61 and 0.15, respectively. The computed results on the fullerene fragments are given in the following sections.

3.1 Molecular Orbitals

Molecular orbitals (MO's) of C_{60} are highly degenerate due to its high symmetry I_h, as shown in Figure 2(*a*) for the vicinity of the HOMO – LUMO gap. As described above, important MO's pertinent to the lowest–allowed transition $1^1A_g \rightarrow 1^1T_{1u}$ are those of the highest occupied h_u–shell and the lowest unoccupied t_{1g}– and h_g–shells. The h_u– shell and h_g–shell are 5–fold degenerate, and the t_{1g}–shell is 3–fold degenerate.

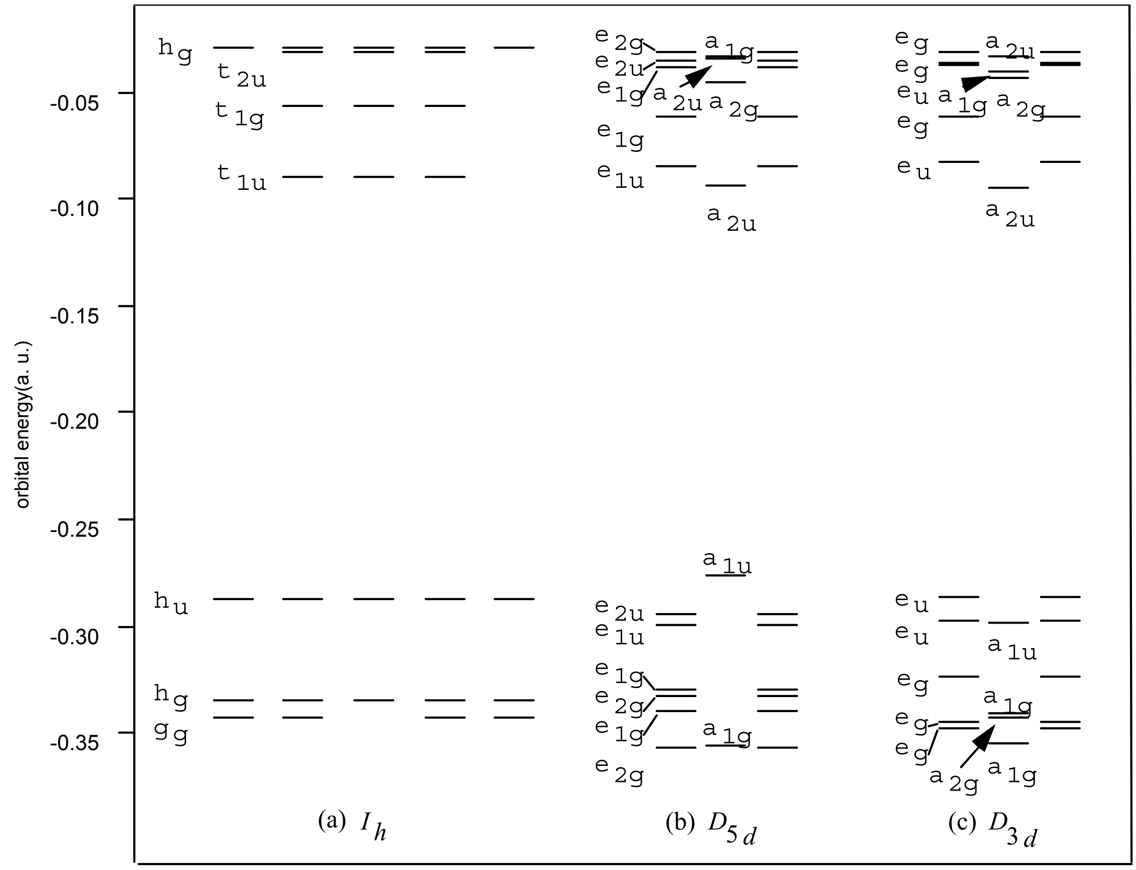

Figure 2. MO–energy levels of C_{60} in the vicinity of the HOMO–LUMO gap, calculated in the CNDO/S approximation. (*a*) The $I_h - C_{60}$, with two CC bond lengths of 1.397 and 1.449Å; (*b*) The elongated $D_{5d} - C_{60}$ (see the text for details); (*c*) The elongated $D_{3d} - C_{60}$ (see the text for details).

To see how these MO–energy levels of C_{60} split as the symmetry breaks from I_h to D_{5d} and D_{3d}, we made SCF–MO calculations on two slightly elongated C_{60} molecules, $D_{5d} - C_{60}$ and $D_{3d} - C_{60}$. The $D_{5d} - C_{60}$ molecule is a C_{60} molecule elongated along the C_5–axis of the D_{5d} symmetry in such a way that its upper corannulene cap of 20 C–atoms and its lower cap of 20 C–atoms are all shifted by +0.1 Å and –0.1 Å, respectively, leaving the central belt of 20 C–atoms unaltered. The $D_{3d} - C_{60}$ molecule is another C_{60} molecule elongated along the C_3–axis of the D_{3d} symmetry in such a way that the upper triphenylene–derivative cap of 24 C–atoms and the lower cap of 24 C–atoms are all shifted by +0.1 Å and –0.1 Å, respectively, leaving the central belt of 12 C–atoms unaltered. The Figure 2 shows the MO–energy levels of these two elongated C_{60} molecules.

In Figure 2, we see that five degenerate MO's in the highest occupied h_u–shell of the $I_h - C_{60}$ molecule split into the highest occupied a_{1u}–MO and two occupied e_{2u}– and e_{1u}–shells as the symmetry breaks from I_h to D_{5d}. Also, three MO's in the lowest unoccupied t_{1g}–shell split into the lowest unoccupied e_{1g}– and a_{2g}–shells, and five MO's in the lowest unoccupied h_g–shell split into the e_{1g}–, a_{1g}–, and e_{2g}–shells. Similarly, we see that the five degenerate HOMO's of the $I_h - C_{60}$ molecule split into the two highest occupied e_u–shells and the highest occupied a_{1u}–shell as the symmetry breaks from I_h to D_{3d}. Also, three MO's in the lowest unoccupied t_{1g}–shell split into the lowest unoccupied e_g– and a_{2g}–shells, and five MO's in the lowest unoccupied h_g–shell split into the a_{1g}–shell and the two e_g–shells.

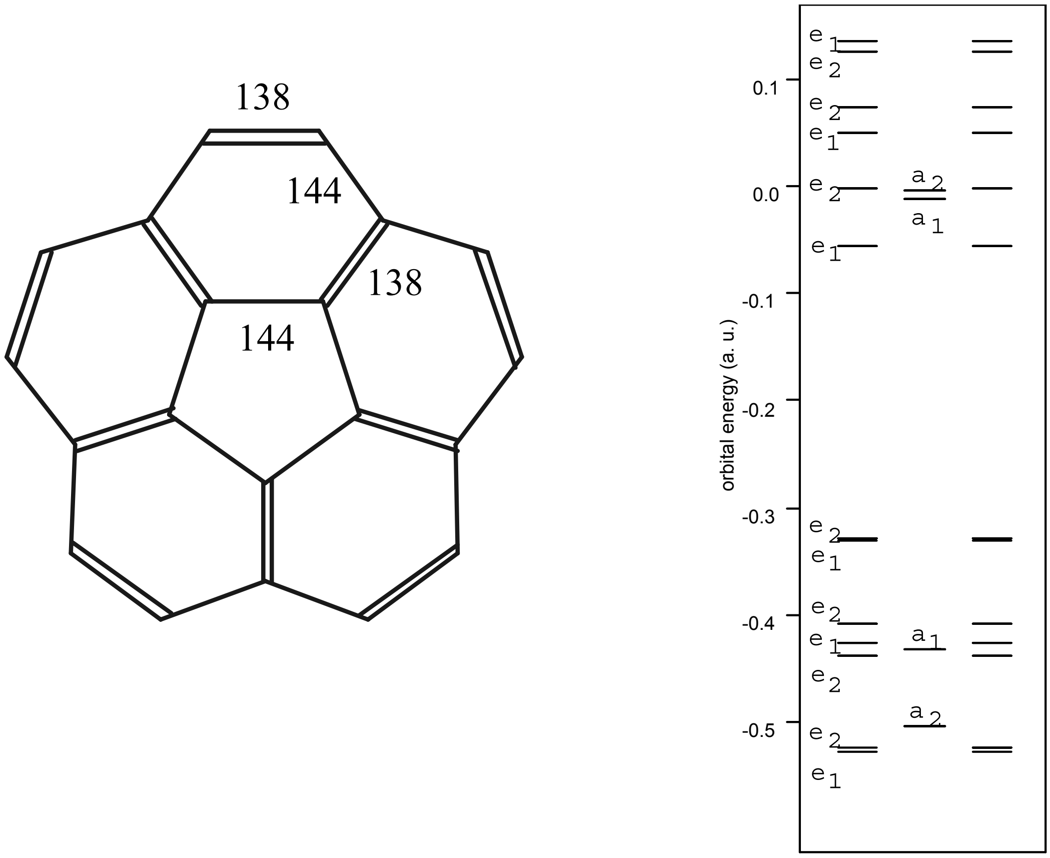

(a) (b)

Figure 3. (*a*) Corannulene and (*b*) its MO–energy levels in the vicinity of the HOMO – LUMO gap, calculated in the CNDO/S approximation. The geometry was determined with MacSpartan at the AM1 level. The CC bondlengths are given in nm.

MO–energy levels of corannulene are shown in Figure 3. The geometrical structure determined with MacSpartan at the AM1 level was used for the SCF–MO calculation. The most striking difference from Figure 2(*b*) in the corresponding MO's is that the highest occupied a_{1u}–MO of D_{5d} – C_{60} is missing in corannulene. In fact, we have found that this a_{1u}–MO of D_{5d} – C_{60} is practically localized at the 20 C–atoms in the equatorial zone, *i.e.*, at the encircled *cis*–polyene of ten ethylene units. This indicates that corannulene alone can not provide all the components of the highest occupied h_u–shell of C_{60}.

The SCF–MO calculations were made on triphenylene and two derivatives whose structures are shown in Figure 4. Model 1, triphenylene, is a planar molecule with symmetry D_{3h}. Model 2 is a bowl–shaped triphenylene derivative, bridged with methylene forming three 5–membered rings between phenyl groups. Model 3 is a radialene with three ethylene groups at vertices of 5–membered rings of Model 2.

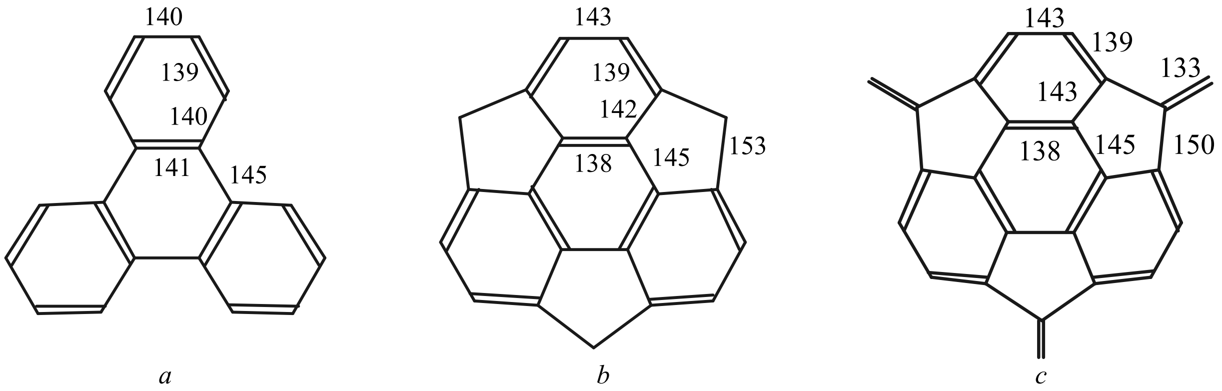

Figure 4. Triphenylene (Model 1) and two derivatives (Models 2 and 3). (*a*) Model 1 (planar: D_{3h}); (b) Model 2 (methylene–bridged, bowl–shaped: C_{3v}); and (*c*) Model 3 (methylene–bridged radialene, bowl–shaped: C_{3v}). The geometrical structures were determined with MacSpartan at the AM1 level. The CC bond lengths are given in nm.

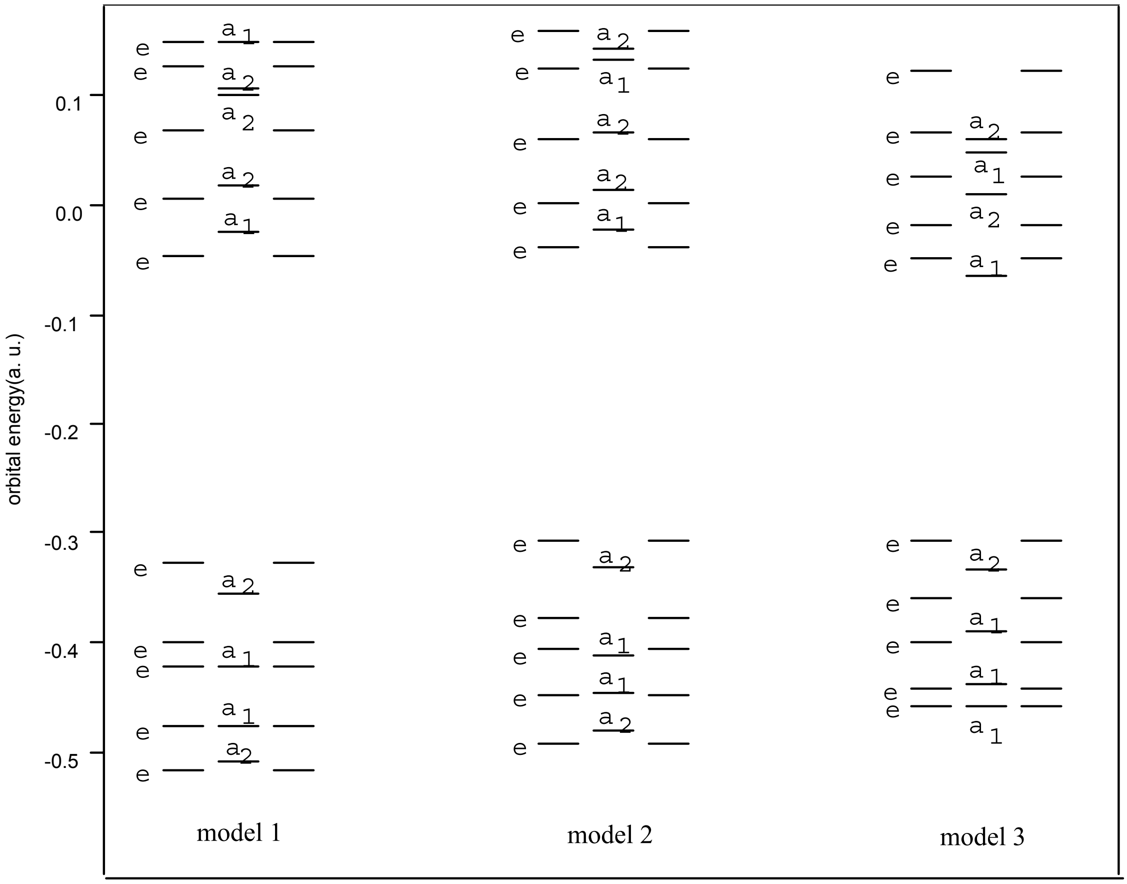

Figure 5. MO–energy levels in the vicinity of the HOMO–LUMO gap, calculated in the CNDO/S approximation. Symbols classifying the energy levels denote the irreducible representations of C_{3v}. Compare these levels with those in Figure 2(*c*) for $D_{3d} - C_{60}$.

Figure 5 shows the MO–energy levels of Models 1, 2 and 3 in the regions of the HOMO–LUMO gaps, calculated in the CNDO/S approximation. On the contrary to corannulene, all MO components of the original C_{60} are found in Models 1–3. This may be clarified by comparing these energy levels with those in Figure 2(*c*) for the elongated D_{3d} – C_{60} molecule. The pattern of the energy levels in the region near the HOMO – LUMO gap becomes more like the one of D_{3d} – C_{60} as the system becomes larger from Model 1 to Model 3. The lowest unoccupied shell of Model 3 is non–degenerate just as the one of D_{3d} – C_{60}, although the highest occupied shells are all doubly degenerate for the three Models 1–3 and D_{3d} – C_{60}.

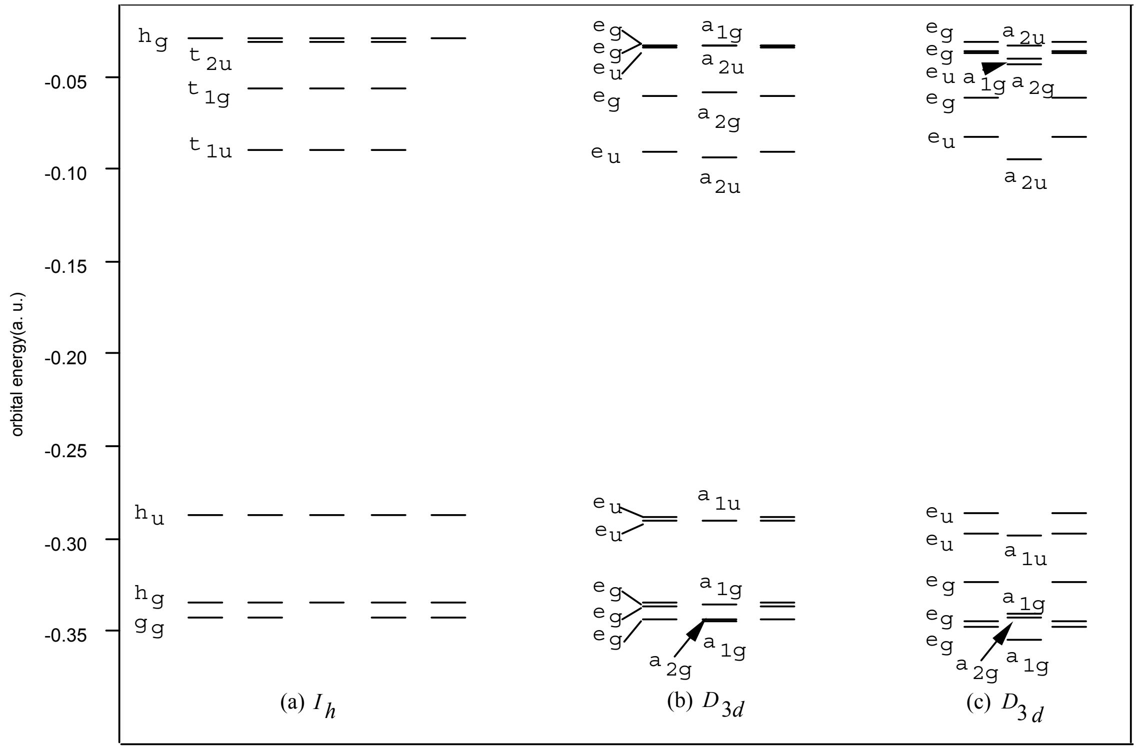

Figure 6. MO–energy levels of (*a*) the I_h – C_{60}, (*b*) the D_{3d} – C_{60} molecule with the cap separation increased by 0.02Å, and (*c*) the D_{3d} – C_{60} molecule with the cap separation increased by 0.2Å which is the same as Figure 2(*c*).

Figure 6 shows how MO–energy levels of C_{60} split as the symmetry breaks from *Ih* to D_{3d} in the vicinity of the HOMO–LUMO gap. The figures (*a*) and (*c*) in Figures 6 are the same as those in Figure 2. Figure 6(*b*), however, shows MO–energy levels of only a very slightly elongated D_{3d} – C_{60} molecule in which the separation between the upper and lower caps is increased only by 0.02 Å from the spherical one rather than by 0.2 Å in the D_{3d} – C_{60} molecule for Figure 6(*c*). It is then clear, for instance, that the two closely lying unoccupied MO's of a_{2g} and a_{1g} in Figure 6(*c*) are originating from the unoccupied t_{1g}– and h_g–shells of the C_{60}, respectively.

3.2 Excitation Energies and Oscillator Strengths

The C_{3v} symmetry is assumed for triphenylene and its derivatives in our group–theoretical analysis, so that the electronic transitions from their ground states ($^1A_1$) are allowed only to the ^1E states. Pairs of these molecules in the staggered conformation take the D_{3d} symmetry, and their allowed transitions are from the $^1A_{1g}$ ground state to the ^1E_u states. Table 1 shows the computed spectra, i.e., the excitation energies (ΔE /eV) and oscillator strengths (f) for some lowest allowed transitions of these molecules (Models 1, 2, and 3). The f–values in Table 1 are doubled for two components of the ^{1}E states. Only those of the excitation energies less than 5 eV are shown here. Table 1 also shows primitive excitations between occupied and unoccupied shells and their weights for each of the $1^1A_1 \rightarrow n^1E$ transitions.

Table 1. Excitation Energies (ΔE in eV, and Wavelengths λ in nm), Oscillator Strengths (f), and Their Primitive Excitations with the Weights for the Allowed $1^1A_1 \rightarrow n^1E$ Transitions of Triphenylene and Its Derivatives.

Model	n	ΔE	λ	f	weight [primitive excitations] [a]
1	1	4.40	282	0.708	0.26 [$e \rightarrow a_1$], 0.19 [$e \rightarrow e$], 0.17 [$a_2 \rightarrow e$],
	2	4.50	276	0.040	0.32 [$e \rightarrow a_1$], 0.25 [$a_2 \rightarrow e$], 0.15 [$e \rightarrow 2e$]
	3	4.80	259	1.905	0.67 [$e \rightarrow e$], 0.07 [$a_2 \rightarrow e$]
2	1	3.74	332	0.295	0.36 [$e \rightarrow e$], 0.19 [$a_2 \rightarrow e$], 0.15 [$e \rightarrow a_1$], 0.09 [$e \rightarrow 2e$]
	2	3.90	318	0.106	0.47 [$e \rightarrow a_1$], 0.10 [$a_2 \rightarrow e$], 0.09 [$e \rightarrow a_2$]
	3	4.36	284	0.915	0.41 [$e \rightarrow e$], 0.24 [$e \rightarrow 2e$], 0.11 [$a_2 \rightarrow e$]
	4	4.59	270	0.006	0.20 [$e \rightarrow a_2$], 0.19 [$a_2 \rightarrow e$], 0.15 [$e \rightarrow a_1$], 0.08 [$e \rightarrow 2e$]
3	1	3.23	384	0.065	0.76 [$e \rightarrow a_1$], 0.05 [$a_2 \rightarrow e$], 0.05 [$2e \rightarrow e$]
	2	3.69	336	0.434	0.28 [$a_2 \rightarrow e$], 0.27 [$e \rightarrow e$], 0.13 [$e \rightarrow 2e$]
	3	3.93	315	1.156	0.43 [$e \rightarrow e$], 0.20 [$e \rightarrow 2e$], 0.09 [$2e \rightarrow a_1$], 0.06 [$a_2 \rightarrow e$]
	4	4.44	279	0.112	0.20 [$e \rightarrow a_2$], 0.15 [$a_2 \rightarrow e$], 0.13 [$e \rightarrow 2e$], 0.06 [$a_2 \rightarrow 2e$]
	5	4.87	255	0.580	0.34 [$2e \rightarrow a_1$], 0.12 [$2e \rightarrow e$], 0.12 [$2e \rightarrow e$], 0.11 [$3e \rightarrow a_1$], 0.07 [$e \rightarrow 2e$]

[a] [$e \rightarrow a_1$], for instance, denotes primitive transitions from the highest occupied (HO) e–shell to the lowest unoccupied (LU) a_1–shell. 2e stands for the 2nd LU or the 2nd HO e–shell. Primitive excitations with the weight of less than 0.05 are not shown.

The first allowed transition of Model 3, the largest Model, has the excitation energy 3.23 eV and the oscillator strength 0.065. We identify this as the very origin of the lowest–allowed transition $1^1A_g \rightarrow 1^1T_{1u}$ of C_{60} that was found in our SECI calculation [4] at 3.47 eV (357 nm) with the oscillator strength $f = 0.34$. The excitation energy 3.23 eV is a little lower, but the value is adjustable according to the way of dealing with the correlation energy of the ground state. The oscillator strength 0.065 should be at least doubled for a pair of the two caps in the D_{3d} staggered conformation. Furthermore, as there are ten choices of such a pair, this should be even more multiplied although one should realize that the pair of the Model 3 molecules already amounts to 2×24 C–atoms, 80% of C_{60}. It is important that 76% of this allowed transition of Model 3 is due to primitive excitations between the highest occupied e–shell and the lowest unoccupied a_1–MO.

The highest occupied e–shell and a_2–MO of Model 3 should give the e_u– and e_g–shells and the a_{1u}– and a_{2g}–MO's, respectively, when the molecules are paired in the D_{3d} conformation. Similarly the lowest unoccupied a_1–MO and e–shell should give the a_{2u}– and a_{1g}–MO's and the e_u– and e_g–shells, respectively. On the other hand, as clearly seen in Figure 6 by comparing (*a*) and (*b*), the highest occupied h_u–shell of C_{60} consists of the occupied a_{1u}–MO and two e_u–shells, and the lowest unoccupied h_g–shell consists of the unoccupied a_{1g}–MO and two e_g–shells. Similarly, the lowest unoccupied t_{1g}–shell consists of the unoccupied a_{2g}–MO and e_g–shell. Therefore, the primitive excitations between the highest occupied e–shell and the lowest unoccupied a_1–MO in the Model 3 molecule are equivalent to those between the highest occupied h_u–shell and the lowest unoccupied h_g–shell of C_{60}. It is rather disappointing that the unoccupied one here is found to be the h_g–shell, but not the t_{1g}–shell as was expected from our SECI calculation on C_{60}. Figure 6 shows how the unoccupied a_{2g}–level and a_{1g}–level emerge from the original t_{1g}–level and h_g–level of C_{60}, respectively, as the two triphenylene–like caps in the northern and southern hemispheres are separated. The unoccupied a_{2g}–level moves up while the unoccupied a_{1g}–level moves down, suggesting that they would reverse the order at a larger separation of the two caps. In fact, the unoccupied a_1–level lies below the a_2–level in Models 1–3 as shown in Figure 5. This suggests that the D_{3d} model of triphenylene–like caps can be improved for the origin of the lowest–allowed absorption band of C_{60} if the interactions between the cap molecules are taken into account. This study is currently proceeding.

4 CONCLUSIONS

We have shown that the lowest–allowed absorption band of C_{60} is fairly well explained in terms of the allowed transitions of its triphenylene–like partial structures. The model can be improved by taking into account the interactions between the two triphenylene–like caps in the staggered D_{3d} conformation. On the contrary, if one tries to explain the absorption band of C_{60} using its corannulene–like partial structures, one must also include the encircled *cis*–polyene of ten ethylene units at its equatorial belt. This is due to the fact that corannulene lacks one component of the HOMO's of C_{60} that belongs to the encircled *cis*–polyene.

The Ih – C_{60} molecule has only two different CC bond lengths. In our calculations we often use 1.397 and 1.449 Å [17]. Note that the CC bond length of ethylene is 1.337 Å and that of ethane is 1.534 Å, while that of benzene is 1.397 Å [18]. The shorter bond length of C_{60} appears to be the same as the CC bond length of benzene, but this is a pure coincidence and does not mean the π–conjugation as strong as benzene. We should make rather emphasis on the existence of the bond alternation in C_{60}.

The fact that the shorter bond length is a little longer than the C=C bond length of ethylene and the longer one is a little shorter than the C–C bond length of ethane reflects the π–conjugation to a certain extent. The whole network of C_{60} consists of 30 shorter CC–bonds and 60 longer CC–bonds. We can therefore visualize the π–conjugation system of C_{60} as a supermolecular system of 30 ethylene units placed on a circumscribing sphere. There are, however, certain ways of coupling among these ethylene units that lead to various low–lying electronic transitions of C_{60}. In the present study, we have shown that the triphenylene–like network leads to the lowest–allowed absorption band of C_{60}. Super aromaticity of fullerenes was recently discussed in a review article [19].

5 REFERENCES

[1] H. W. Kroto, J. R. Heath, S. C. O'Brien, R. F. Curl, and R. E. Smalley, C_{60}: Buckminsterfullerene, *Nature* **1985**, *318*, 162–163.

[2] L. T. Scott, P.–C. Cheng, M. M. Hashemi, M. S. Bratcher, D. T. Meyer, and H. B. Warren, Corannulene. A Three–Step Synthesis, *J. Am. Chem. Soc.* **1997**, *119*, 10963–10968.

[3] L. T. Scott, M. M. Boorum, B. J. McMahon, S. Hagen, J. Mack, J. Blank, H. Wegner, and A. de Meijere, A Rational Chemical Synthesis of C_{60}, *Science* **2002**, *295*, 1500–1503.

[4] T. Hara, S. Narita, S. Kumei, and T. Shibuya, Complete TDA and RPA Calculations on the Electronic Transitions of Fullerene–C_{60} in the CNDO/S and INDO/S Approximations, *Int. J. Quantum Chem.* **2001**, *85*, 136–161.

[5] J. Del Bene and H. H. Jaffe, Use of the CNDO Method in Spectroscopy. I. Benzene, Pyridine, and the Diazines, *J. Chem. Phys.* **1968**, *48*, 1807–1813.

[6] J. Del Bene and H. H. Jaffe, Use of the CNDO Method in Spectroscopy. II. Five–Membered Rings, *J. Chem. Phys.* **1968**, *48*, 4050–4055.

[7] J. Del Bene and H. H. Jaffe, Use of the CNDO Method in Spectroscopy. III. Monosubstituted Benzenes and Pyridines, *J. Chem. Phys.* **1968**, *49*, 1221–1229.

[8] J. Del Bene and H. H. Jaffe, Use of the CNDO Method in Spectroscopy. IV. Small Molecules: Spectra and Ground–State Properties, *J. Chem. Phys.* **1969**, *50*, 1126–1129.

[9] R. L. Ellis, G. Kuehnlenz,, and H. H. Jaffe, Use of the CNDO Method in Spectroscopy. VI. Further $n\pi^*$ Transitions, *Theoret. Chim. Acta* **1972**, *26*, 131–140.

[10] Spartan ver. 5.0 programs for the Power Macintosh, Wavefunction, Inc., 18401 Von Karman, Suite 370, Irvine, CA 92612, USA.

[11] M. J. S. Dewar, E. G. Zoebisch, E. F. Healy, and J. J. P. Stewart, AM1: A New General Purpose Quantum Mechanical Molecular Model, *J. Am. Chem. Soc.* **1985**, *107*, 3902–3909.

[12] J. A. Pople, D. L. Beveridge, and P. A. Dobosh, Approximate Self–Consistent Molecular–Orbital Theory. V. Intermediate Neglect of Differential Overlap, *J. Chem. Phys.* **1967**, *47*, 2026–2033.

[13] H. Ito, H. Kameshima, and T. Shibuya, Equations–of–Motion Method for the Spin–Orbit Coupling of Aromatic Molecules: Application to the Phosphorescence Lifetime of Benzene, *J. Chem. Phys.* **1996**, *104*, 1309–1324.

[14] J. E. Ridley and M. C. Zerner, Intermediate Neglect of Differential Overlap (INDO) Technique for Spectroscopy. Pyrrole and the Azines, *Theoret. Chim. Acta* **1973**, *32*, 111–134.

[15] J. D. Baker and M. C. Zerner, Applications of the Random–Phase Application with the INDO/S Hamiltonian: UV–VIS Spectra of Free Base Porphin, *Chem. Phys. Lett.* **1990**, *175*, 192–196.

[16] J. Feng, J. Li, Z. Wang, and M. C. Zerner, Quantum–Chemical Investigation of Buckminsterfullerene and Related Carbon Clusters (I): The Electronic Structure and UV Spectra of Buckminsterfullerene, and Other C_{60} Cages, *Int. J. Quantum Chem.* **1990**, *37*, 599–607.

[17] T. Shibuya and M. Yoshitani, Two Icosahedral Structures for the C_{60} Cluster, *Chem. Phys. Lett.* **1987**, *137*, 13–16.

[18] Nihon Kagaku–Kai (The Chemical Society of Japan) (Ed.), *Kagaku Benran* (*Handbook of Chemistry*), *2nd Ed.*, Maruzen, Tokyo, 1975 (in Japanese).

[19] M. Buehl and A. Hirsch, Spherical Aromaticity of Fullerene, *Chem. Rev.* **2001**, *101*, 1153–1183.

Biographies

Tai–ichi Shibuya is professor of chemistry at the Faculty of Textile Science and Technology, Shinshu University. He obtained a Ph.D. degree in physical chemistry from Yale University. His major research field is quantum chemistry.

Susumu Narita is associate professor of chemistry at the Faculty of Textile Science and Technology, Shinshu University. He obtained a Ph.D. degree in chemistry from Tokyo University of Education. His research field is computational chemistry.

Yasushi Nomura is assistant professor of chemistry at the Faculty of Textile Science and Technology, Shinshu University. He obtained a Ph.D. degree in chemistry from Tohoku University. His research field is quantum chemistry.

Tetsuo Morikawa is professor of chemistry at Joetsu University of Education. He obtained a Ph.D. degree in chemistry from Tokyo University of Education. His research field is theoretical chemistry with graph theory.